Tumor growth suppression by the combination of nanobubbles and ultrasound

Ryo Suzuki,[1] Yusuke Oda,[1] Daiki Omata,[1] Norihito Nishiie,[1] Risa Koshima,[1] Yasuyuki Shiono,[1] Yoshikazu Sawaguchi,[2] Johan Unga,[1] Tomoyuki Naoi,[1] Yoichi Negishi,[3] Shigeru Kawakami,[4] Mitsuru Hashida[5,6] and Kazuo Maruyama[1]

[1]Laboratory of Drug Delivery System, Faculty of Pharma-Sciences, Teikyo University, Tokyo, Japan; [2]Nihon Pharmaceutical University, Saitama, Japan; [3]Department of Drug Delivery and Molecular Biopharmaceutics, School of Pharmacy, Tokyo University of Pharmacy and Life Sciences, Tokyo, Japan; [4]Department of Pharmaceutical Informatics, Department of Clinical Pharmacy, Graduate School of Biomedical Sciences, Nagasaki University, Nagasaki, Japan; [5]Department of Drug Delivery Research, Graduate School of Pharmaceutical Sciences, Kyoto University, Kyoto, Japan; [6]Institute of Integrated Cell-Material Sciences, Kyoto University, Kyoto, Japan

We previously developed novel liposomal nanobubbles (Bubble liposomes [BL]) that oscillate and collapse in an ultrasound field, generating heat and shock waves. We aimed to investigate the feasibility of cancer therapy using the combination of BL and ultrasound. In addition, we investigated the anti-tumor mechanism of this cancer therapy. Colon-26 cells were inoculated into the flank of BALB/c mice to induce tumors. After 8 days, BL or saline was intratumorally injected, followed by transdermal ultrasound exposure of tumor tissue (1 MHz, 0–4 W/cm^2, 2 min). The anti-tumor effects were evaluated by histology (necrosis) and tumor growth. *In vivo* cell depletion assays were performed to identify the immune cells responsible for anti-tumor effects. Tumor temperatures were significantly higher when treated with BL + ultrasound than ultrasound alone. Intratumoral BL caused extensive tissue necrosis at 3–4 W/cm^2 of ultrasound exposure. In addition, BL + ultrasound significantly suppressed tumor growth at 2–4 W/cm^2. *In vivo* depletion of CD8$^+$ T cells (not NK or CD4$^+$ T cells) completely blocked the effect of BL + ultrasound on tumor growth. These data suggest that CD8$^+$ T cells play a critical role in tumor growth suppression. Finally, we concluded that BL + ultrasound, which can prime the anti-tumor cellular immune system, may be an effective hyperthermia strategy for cancer treatment.

High-intensity focused ultrasound (HIFU) is a non-invasive therapy commonly used to destroy a targeted area without damaging the surrounding tissue.[1,2] This thermal ablation therapy has been applied to various diseases, including tumor ablation in the liver, bladder, uterus and prostate.[3–6] However, there are some limitations regarding the clinical application of HIFU for cancer therapy.[7] First, several HIFU exposures are required to ablate the entire volume because the focal point is only a few square millimeters. Second, sufficient cooling time must be allowed between applications to prevent the ablation of normal tissue surrounding the tumor. Consequently, HIFU treatments involve multiple long sessions that are uncomfortable for the patients.[8] In addition, HIFU is currently not approved for breast cancer because it causes skin burns around shallow tumors.[2] Most adverse effects are caused by the high acoustic intensity of HIFU. However, the use of lower acoustic power or shorter time exposure would reduce treatment efficacy.

Recent improvements to ultrasound therapy include combinations of HIFU/non-focused ultrasound with microbubbles, nanobubbles or nanodroplets.[9–11] These bubbles (and droplets after phase changing of nanodroplets) oscillate under lower

acoustic power. Thereby, a part of the ultrasound energy is absorbed and changed to heat. Higher acoustic power may lead to collapse of bubbles. This phenomenon, known as cavitation, induces jet streams, heat and the generation of reactive oxygen species,[12–14] thereby damaging nearby cells. When ultrasound without a focal point is used to irradiate a tissue, the chemical, thermal and mechanical effects are mild compared to HIFU. To enhance these effects with a non-focused ultrasound system, the combination of bubbles and non-focused ultrasound has been studied. Nano-bubbles or micro-bubbles oscillate and disrupt in an ultrasound field, inducing various effects as mentioned above. Generally, these effects can be induced even at low intensity of ultrasound, which has a very small effect without bubbles. Therefore, it is thought that for non-focused ultrasound exposure in the absence of bubbles, there is low risk of tissue damage. Recently, the combination of bubbles and ultrasound has been utilized in thrombosis systems[15,16] and gene/drug delivery systems.[17,18] In the field of thermal effects, it was reported that intravenous administration of microbubbles caused a fivefold increase in murine kidney temperature during ultrasound exposure.[10] We recently developed Bubble liposomes (BL) entrapping perfluoropropane gas

nanobubbles.[19–22] There are various medical applications for these small and stable BL, such as contrast imaging agents and drug and gene delivery.[20,22] Moreover, we reported that intra-tumoral injection of BL enhances the anti-tumor effect of HIFU in mice.[23] In the present study, we tested the potential of intratumoral BL and ultrasound (≤ 4 W/cm^2) as an effective cancer therapy with reduced adverse effects. In addition, in physical cancer therapies such as radiotherapy and photodynamic therapy, it is suggested that their anti-tumor effects are associated with priming of the systemic immune system for cancer cells.[24] Moreover, low-pressure pulsed focused ultrasound with microbubbles promoted immune cell infiltrations.[25] Therefore, we hypothesized that the combination of intratumoral injection of BL and ultrasound would enhance the anti-tumor effect through a mechanism involving anti-tumor immune responses. In this study, we also studied the effect of cellular immunity on the therapeutic efficacy of BL + ultrasound.

Materials and Methods

Cells and animals. Murine colon adenocarcinoma Colon-26 cells were purchased from RIKEN Cell Bank. Colon-26 cells were grown in RPMI-1640 (Wako Pure Chemical Industries, Osaka, Japan) containing 100 U/mL penicillin (Wako Pure Chemical Industries) and 100 μg/mL streptomycin (Wako Pure Chemical Industries) supplemented with 10% heat-inactivated FBS (Life Technologies, Carlsbad, CA, USA). BALB/c female mice were obtained from Sankyo Labo Service (Tokyo, Japan) and used at 6 weeks of age. All of the experimental procedures were performed in accordance with the Teikyo University guidelines for the welfare of animals in studies of experimental neoplasia.

Preparation of the Bubble liposomes. Liposomes composed of 1,2-distearoyl-sn-glycero-phosphatidylcholine (DSPC) (NOF, Tokyo, Japan) and N-(Carbonyl-methoxypolyethyleneglycol 2000)-1,2- distearoyl-sn-glycero-3-phosphatidylethanolamine (DSPE-PEG(2k)-OMe) (PEG, Mw = ca. 2000) (NOF) (94:6 [mol/mol]) were prepared by reverse-phase evaporation.[19] In brief, all reagents (total lipid: 100 μmol) were dissolved in 8 mL of 1:1 (v/v) chloroform/diisopropyl ether. A total of 4 mL of PBS was added, and the mixture was sonicated and evaporated at 65°C. The organic solvent was completely removed, and the size of the liposomes was adjusted to <200 nm using an extruding apparatus (Northern Lipids, Vancouver, BC, Canada) and sizing filters (pore sizes: 100 and 200 nm [Nuclepore Track-Etch Membrane, Whatman, UK]). After sizing, the liposomes were sterilized through a 0.45-μm pore size filter (Millex HV filter unit; Durapore PVDF membrane, Millipore, MA, USA). The diameter of the liposomes (150–200 nm) was measured by dynamic light scattering (ELS-800; Otsuka Electronics, Osaka, Japan). The lipid concentration was measured with an HPLC system (Hitachi High-Technologies, Tokyo, Japan) and an Evaporative Light Scattering Detector (ASTECH, Tokyo, Japan). The BL were prepared using the liposomes and perfluoropropane (Takachiho Chemical Industrial, Tokyo, Japan). In brief, 5-mL sterilized vials (Maruemu, Osaka, Japan) containing 2 mL of liposome suspension (lipid concentration: 1 mg/mL) were filled with perfluoropropane, capped and supercharged with 7.5 mL of perfluoropropane. The vial was placed in a bath-type sonicator (42 kHz, 100 W; Bransonic 2510J-DTH, Branson Ultrasonics, Danbury, CT, USA) for 5 min to form BL. The liposomes were reconstituted by sonication and supercharged with

perfluoropropane in the vial. Perfluoropropane was entrapped within the lipid micelles, comprising DSPC and DSPE-PEG (2k)-OMe, to form nanobubbles. The perfluoropropane gas nanobubbles were encapsulated within the reconstituted liposomes. The mean diameter of these BL was approximately 500 nm.

Ultrasound exposure in vivo. Sonitron 2000V (Nepa Gene, Chiba, Japan) was utilized as a device for ultrasound exposure in in vivo experiments. This device generates ultrasound from a non-focused ultrasound transducer (diameter 12 mm). Mechanical index (MI) values utilized in our study were 0.147, 0.207, 0.254 and 0.283 for acoustic intensity of 1, 2, 3 and 4 W/cm^2, respectively, in 1 MHz. Root mean squared averages of sound peak pressure were 0.109, 0.154, 0.188 and 0.217 MPa, respectively. These values were supplied from Nepa Gene.

Tumor inoculation. BALB/c mice were subcutaneously inoculated with Colon-26 tumor cells (1×10^6 cells/mouse) into the flank. After 8 days, we utilized these mice in this experiment as tumor-bearing mice.

Measurements of tumor temperature. Tumor temperature was measured with a thermocouple (RIC-410; GRAPHTEC, Kanagawa, Japan) and data logger (midi LOGGER; GRAPHTEC). First, the thermocouple was inserted into the center of the tumor tissue of anesthetized tumor-bearing mice. Second, a suspension of BL (0.1 mg/mL, 30 μL/mouse) or saline at room temperature was intratumorally injected at the upper side of the thermocouple. Third, ultrasound was transdermally applied via ultrasonic gel (SONOJELLY; Toshiba Medical Supply, Tokyo, Japan) and ultrasound (frequency 1 MHz, duty 50%, burst rate 2.0 Hz, intensity 0–4 W/cm^2) was exposed to the tumor for 2 min. Finally, tumor temperature was recorded at each time point after ultrasound exposure. Under these exposure conditions, no damage to skin or tissue surrounding the tumors was seen.

Histochemical analysis. A suspension of BL (0.1 mg lipid/ mL, 30 μL/mouse or saline was injected into the tumor of tumor-bearing mice, and ultrasound (frequency 1 MHz, duty 50%, burst rate 2.0 Hz, intensity 0–4 W/cm^2) was transdermally applied to the tumor for 2 min. After the mice were killed, the tumor tissue was dissected, fixed with 10% formaldehyde for 24 h, embedded in paraffin wax and cut into 10-μm-thick sections. The sections were stained with hematoxylin and eosin stain (H&E) to evaluate general morphology under a light microscope (IX-71, Olympus, Tokyo, Japan).

Anti-tumor effect. A suspension of BL (0.1 mg/mL, 30 μL) or saline was injected into the tumor and ultrasound (frequency 1 MHz, duty 50%, burst rate 2.0 Hz, intensity 0–4 W/cm^2) was transdermally applied to the tumor for 2 min via ultrasonic gel. The anti-tumor effects were evaluated by measuring tumor volume using the formula: (major axis × minor axis^2) × 0.5.

In vivo **depletion assays.** The GK1.5 hybridoma (rat anti-mouse CD4 mAb) and 53-6.72 hybridoma (rat anti-mouse CD8 mAb) were purchased from the American Type Culture Collection (Manassas, VA, USA). BALB/c nude mice were injected i.p. with each hybridoma, and the ascites were collected to purify antibodies by protein A column (GE Healthcare Japan, Tokyo, Japan). On day 8 after inoculation of Colon-26 tumor cells, mice were intratumorally injected with BL or saline, followed by ultrasound (frequency 1 MHz, duty 50%, burst rate 2.0 Hz, intensity 4 W/cm^2). In addition, mice received 2 *i.p.* injections (days 5 and 12) of 100 μL/mouse anti-mouse CD8 antibody (CD8$^+$ cells) or anti-mouse CD4

antibody (CD4^{+} cells). Other mice received 5 *i.p.* injections of 200 μL/mouse anti-asialoGM1 mAb (Wako Pure Chemical Industries) (NK cells) on days 5, 6, 7, 8 and 13. Other mice received isotype IgG (normal rat IgG) as a control for antibody injection. Tumor volume was monitored *in vivo* as described above.

Statistical analysis. All animal groups contained four to six mice. The data are expressed as mean ± SD. The different groups were compared with non-repeated measures ANOVA and Dunnett's test. Statistical significance was set at *P* < 0.05.

Results

Heat generation in tumor tissue with Bubble liposomes and ultrasound. *In vivo* studies were conducted with BALB/c mice to test the impact of BL collapse on heat generation in the tumor during ultrasound exposure. Ten days after subcutaneous inoculation of Colon 26 tumor cells, the anesthetized animals were intratumorally injected with BL or saline, followed by ultrasound exposure. Figure 1a shows that tumor temperature gradually increased with ultrasound intensity. In contrast, tumor temperatures were significantly higher in the presence of intratumoral BL, and the overheating effect increased with ultrasound intensity. In the treatment of BL and 4 W/cm^{2} ultrasound exposures, the tumor temperature gradually increased and achieved the plateau at approximately 1.5 min. Finally, this tumor temperature at 2 min with BL + ultrasound was 6°C higher than with saline + ultrasound (Fig. 1b).

Impact of Bubble liposomes ultrasound-mediated tumor damage. Studies were conducted with BALB/c mice to test the impact of BL on tumor damage. Eight days after subcutaneous inoculation of Colon-26 tumor cells, the anesthetized animals were intratumorally injected with BL or saline, followed by ultrasound exposure. Histopathological changes were assessed by H&E staining (Fig. 2). The tumors were not affected by the 2-min ultrasound exposure, regardless of ultrasound intensity. In contrast, the presence of intratumoral BL caused tissue necrosis starting at 3 W/cm^{2}, and even more necrosis at 4 W/cm^{2}.

Bubble liposome enhance the anti-tumor effects of ultrasound exposure. The overall anti-tumor effect of ultrasound exposure was determined for 22 days after BALB/c mice were inoculated with Colon-26 tumor cells. The animals were exposed to ultrasound or a combination of BL and ultrasound on day 8 after inoculation. We first examined an anti-tumor effect with ultrasound alone. There was a tendency toward tumor growth suppression at 1–3 W/cm^{2}, and a weak anti-tumor effect with 4 W/cm^{2} (*P* < 0.05; Fig. 3a), suppressing tumor growth to approximately 70% of the control, a reduction of 30% (Fig. 3c). Second, we examined an effect of intratumoral injection of BL. In the presence of intratumoral BL, significant anti-tumor responses were detected, starting with 2 W/cm^{2}, and increasing with ultrasound intensity (*P* < 0.05 and 0.01; Fig. 3b). At an intensity of 4 W/cm^{2}, the combination of BL and ultrasound suppressed tumor growth by approximately 45% compared with control (non-treatment) animals (Fig. 3d). We also examined the anti-tumor effect by intratumoral BL injection without ultrasound exposure in another experiment. On day 21 after intratumoral BL injection, tumor volume (%) was 109.2 ± 23.8 (mean ± SD, *n* = 5) compared to non-treatment mice, indicating no tumor growth suppression without ultrasound.

The results in Figure 3a and b are from independent experiments. Tumor volume was measured on similar days after
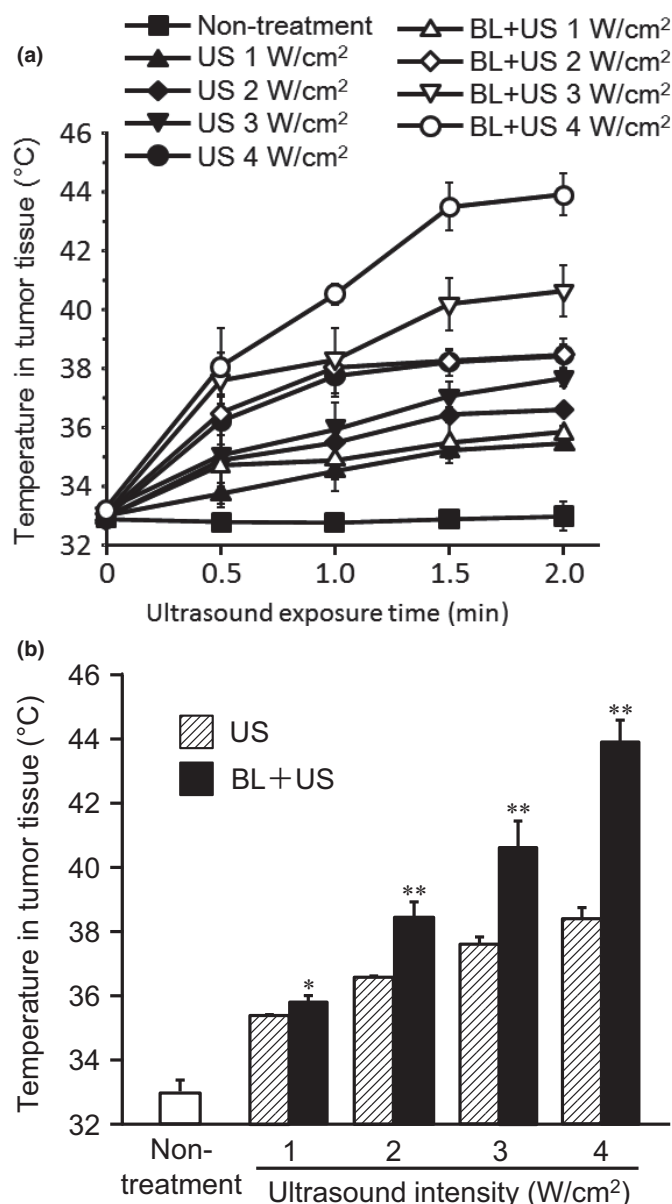

Fig. 1. Tumor temperature after ultrasound exposure with/without BL. BALB/c mice were inoculated with Colon-26 tumor cells in the flank. After 10 days, a thermocouple was inserted in the tumor of the anesthetized mice, followed by intratumoral injection of BL or saline, and ultrasound (0–4 W/cm^{2}, 2 min). (a) Tumor temperature was measured at each time point after ultrasound exposure. (b) The data shows the temperature in tumor tissue at 2 min after ultrasound exposure. The data represent the mean ± SD (*n* = 3). **P* < 0.01 or ***P* < 0.05 for the combination of BL and ultrasound compared with ultrasound. BL, Bubble liposomes; US, ultrasound.

tumor inoculation, but resulted in different tumor volumes. To compare the anti-tumor effects between these experiments, the tumor volumes represented in Figure 3c and d were normalized to control tumors from each experiment.

Immune cells responsible for tumor growth suppression by Bubble liposomes + ultrasound exposure. The combination of BL and ultrasound damaged tumors, suggesting that tumor-associated antigens could be released from the damaged cells and activate immune cells responsible for tumor growth suppression. Therefore, we investigated the involve-
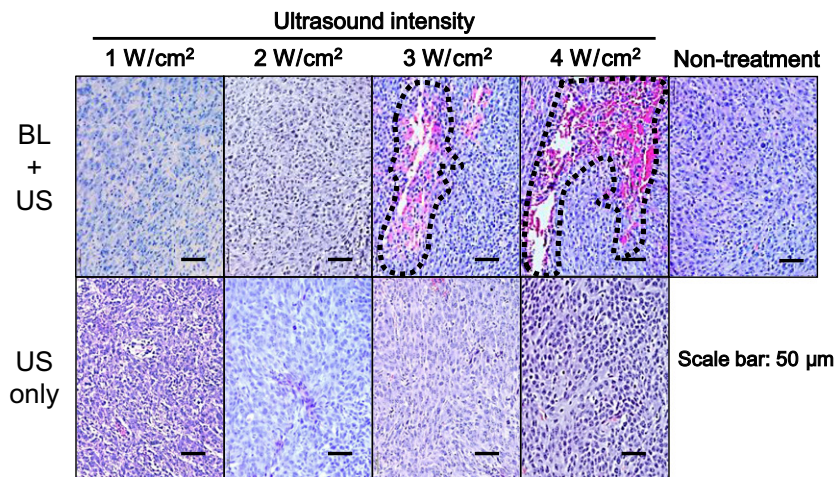
Fig. 2. Histopathology of the tumors after ultrasound exposure with∕without Bubble liposomes (BL). BALB∕c mice were inoculated in the flank with Colon-26 tumor cells. After 8 days, the tumors were treated with intratumoral BL and ultrasound (1–4 W∕cm², 2 min) or ultrasound (0–4 W∕cm², 2 min). Paraffin sections of the tumors were stained with H&E. Necrotic areas (dashed lines) were observed under a light microscope.
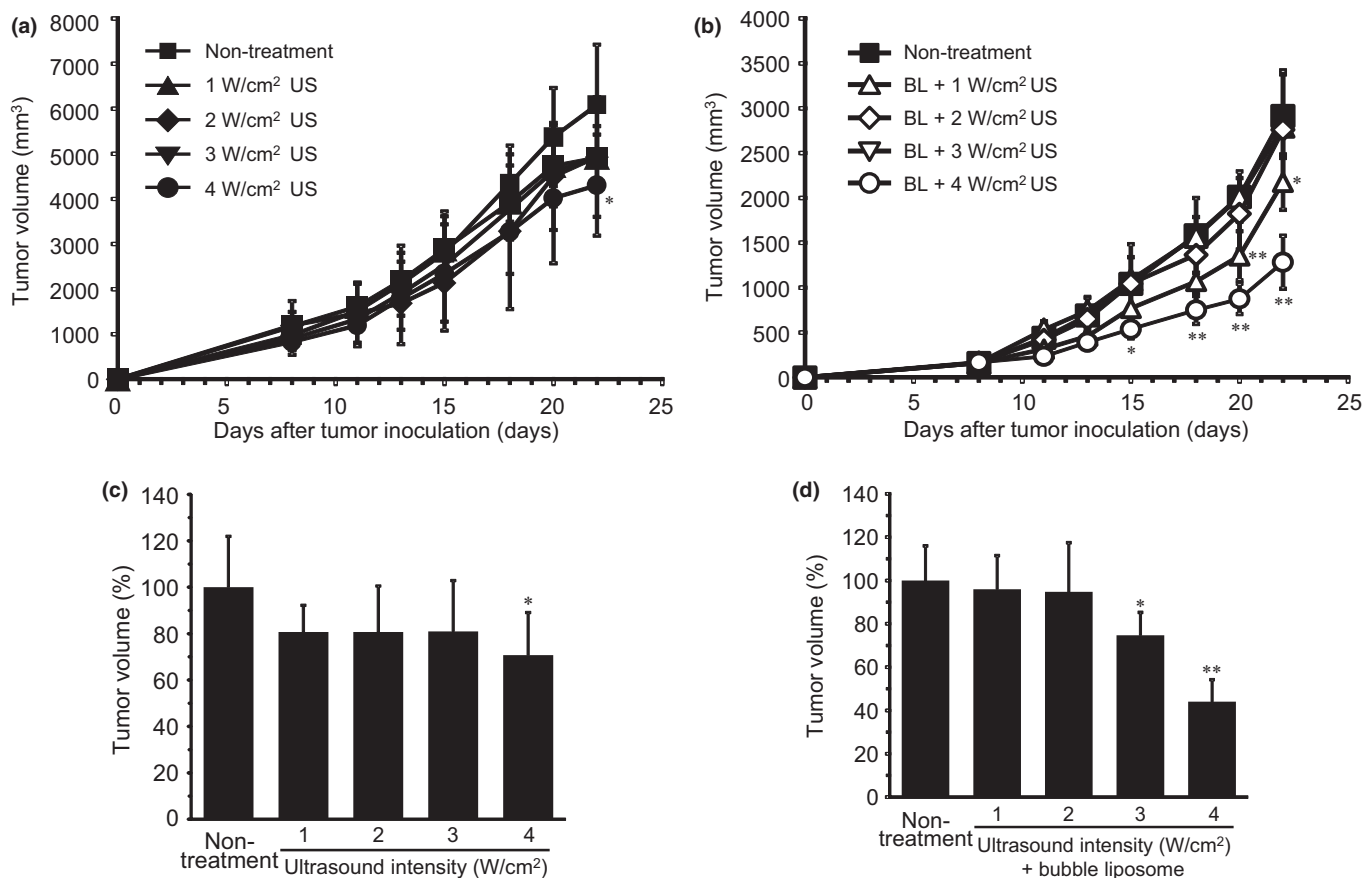

Fig. 3. Tumor growth suppression by ultrasound exposure with∕without BL. BALB∕c mice were inoculated with Colon-26 tumor cells in the flank. After 8 days, the tumors were treated with: (a) ultrasound (0–4 W∕cm², 2 min) or (b) intratumoral BL and ultrasound (1–4 W∕cm², 2 min). Percentage of tumor volume in the treatment of (c) ultrasound alone or (d) BL + ultrasound compared to non-treatment group after 22 days of tumor inoculation. Each point represents the mean ± SD (n = 4,5). **$P < 0.01$ or *$P < 0.05$ compared to non-treatment mice at each time point. BL, Bubble liposomes; US, ultrasound.

ment of immune cells known to play major roles in anti-tumor cellular immunity: $CD4^+$ T cells, $CD8^+$ T cells and NK cells (Fig. 4). Depletion of NK cells or $CD4^+$ T cells did not attenuate the anti-tumor effect of BL + ultrasound exposure. In contrast, the depletion of $CD8^+$ T cells, or $CD4^+$ and $CD8^+$ T cells, effectively blocked the anti-tumor effect of BL + ultrasound. These experiments demonstrate

that $CD8^+$ T cells were the predominant effector cells in this therapeutic response.

Discussion

Nanobubble collapse in ultrasound fields (*i.e.* acoustic cavitation) is an extremely rapid process. This phenomenon leads to
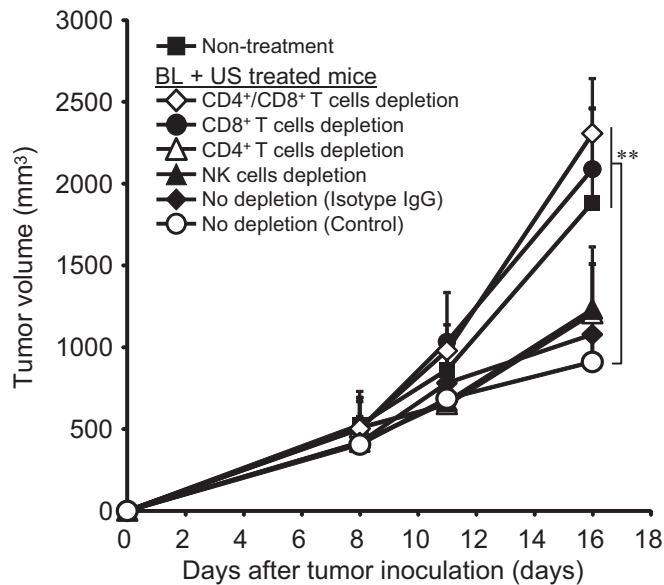
Fig. 4. Identification of the immune cells responsible for tumor growth suppression after exposure to the combination of BL and ultrasound. BALB/c mice were inoculated in the flank with Colon-26 tumor cells. For depletion of CD4+ T cells, CD8+ T cells or NK cells, different mouse groups received i.p. injections of GK1.5 ascites (anti-CD4), 53-6.72 ascites (anti-CD8) or anti-asialoGM1, respectively. Other mice were injected with normal rat IgG as a control for antibody injection. After 8 days, the tumors were treated with intratumoral BL and ultrasound (4 W/cm², 2 min). Tumor volume was monitored. Each point represents the mean ± SD (*n* = 5,6). **P < 0.01 or *P < 0.05 compared with mice with complete immune competent cells (no depletion [control]). BL, Bubble liposomes; US, ultrasound.

localized heating of the bubble interior, which breaks molecular bonds of the gas and vapor. The heat generation has the potential to induce necrosis.[26–28] Therefore, bubble collapse could be an asset for ablative cancer therapies. The present study demonstrates that the injection of BL into the tumor considerably improves the anti-tumor capacity of ultrasound exposure.

First, *in vivo* experiments showed higher tumor temperatures after treatment with a combination of BL and ultrasound than with ultrasound alone and the benefit increased with beam intensity (Fig. 1). Morris *et al.* report additional temperature rise because of friction between the thermocouple and the biological tissue upon ultrasound exposure.[29] In that experiment, a HIFU system was utilized and the ultrasound intensity (1.7 MHz, free-field spatial-peak temporal average intensities 40–600 W/cm²) was much higher than that of our system (1 MHz, acoustic intensity 1–4 W/cm²). Therefore, in our experiment, it is expected that the effect of the friction on temperature rise will be low. In Figure 1, the temperature rise with the combination of BL and ultrasound exposure was higher than that in saline + ultrasound exposure. This difference in temperature should be the result from heat generation due to cavitation of BL. The intratumoral injection of BL has the potential to increase treatment effectiveness. The capacity of BL to generate heat during ultrasound exposure suggests that BL and ultrasound exposure together may induce necrosis (Fig. 2). Therefore, we used a tumor mouse model to test the impact of intratumoral BL on these cell responses. Ultrasound exposure (1–4 W/cm²) did not induce noticeable tissue damage, whereas the combination of BL and ultrasound exposure

caused considerable tumor necrosis. These data suggest that intratumoral injection of BL would improve the anti-tumor effectiveness of ultrasound exposure primarily through tissue necrosis.

The applicability of BL and ultrasound exposure to cancer therapy was tested with regard to the tumor growth rate (Fig. 3). Ultrasound only suppressed tumor growth at the highest intensity of 4 W/cm². The mechanism of this tumor growth suppression is not clear. As shown in Figure 1, temperature in tumor gradually increased with increasing ultrasound intensity also upon treatment with ultrasound exposure alone. Therefore, some tumor cells may be damaged. The combination of BL and ultrasound effectively caused tumor growth suppression starting at 2 W/cm². With BL present, an effect on the tumor growth could be seen at lower ultrasound intensities than without BL and at the same ultrasound intensity a larger effect was achieved with BL. We recently reported that BL can be used for gene delivery under low intensity ultrasound (<1 W/cm²), without cytotoxicity.[20,22] Therefore, low-intensity ultrasound would be preferable for safe gene delivery by BL, whereas higher intensities (2–4 W/cm²) would be more efficient in combination with the combination of BL and ultrasound in cancer therapy. An additional parameter to consider for the anti-tumor effect is BL concentration. We have not optimized the concentration of BL yet. We think that there is an optimal concentration, as in gene delivery, for the combination of BL and ultrasound. At too high a concentration, the BL attenuated the ultrasound beam, which resulted in insufficient cavitation being induced for effective gene delivery. In short, higher concentration of BL disturbs the ultrasound transmission and results in it not being effective in inducing cavitation. Finally, tumor tissue would not be effectively insured under this condition; we should optimize the concentration of BL.

The mechanism of tumor growth suppression was investigated by *in vivo* cell depletion assay because the immune system was implicated in tumor regression during radiation therapy.[30] Local radiation stimulated the production of tumor peptide-reactive IFNγ-producing antitumor immune cells and their trafficking to tumor-draining lymph nodes and tumors. In addition, clinical studies conducted with cancer patients reported that HIFU tumor ablation induces the infiltration of various lymphocyte subsets, including CD4+ and CD8+ T cells, as well as NK cells.[31,32] The combination of BL and ultrasound exposure might induce damage to tumor cells by making pores in cell membrane with mechanical effects such as induction of jet stream associated with cavitation of BL and by thermal effect. Therefore, we hypothesized that this combination of BL and ultrasound exposure may also induce the release of tumor-associated antigens via the pores of the damaged cells that could prime the antitumor immune system. CD8+ T cell depletion and the combination of CD4+ and CD8+ T cell depletion completely inhibited BL + ultrasound-mediated tumor growth suppression (Fig. 4). For these treatment groups, tumor growth was rather enhanced. The reason for the increased tumor growth was most likely suppression of the immune system, in a similar way as seen with immunosuppressive agents. In CD4+ and CD8+ T cells depleted mice, tumor growth was faster than in non-treated mice, indicating that T cell depletion accelerated tumor growth. In another report, the same phenomenon was observed.[33] In contrast, neither CD4+ T cells nor NK cell depletion dramatically inhibited tumor growth suppression. These data are consistent with the essential role

ascribed to CD8^{+} T cells in radiation-mediated tumor growth regression. Furthermore, we showed that this immune response was subset-specific because CD4^{+} T cells and NK cells were not involved in the anti-cancer effect. Altogether, these data show that the anti-tumor effect in BL + ultrasound therapy specifically involves CD8^{+} T cells.

In our combination therapy of BL + ultrasound, tumor tissue was partially destroyed (Fig. 2). Under this condition, tumor cells might leak from the primary tissue into the blood flow and induce metastasis. However, in our case, cellular immune system, especially CD8^{+} T cells, has been induced against cancer cells. Therefore, we expect that this immune system would suppress tumor metastasis. HIFU treatment also destroys tumor tissue and might increase the risk of tumor metastasis due to leaking of tumor cells into the blood flow. However, Xing et al. reported that the HIFU treatment did not increase the risk of distant metastasis.[34] They reported the induction of an anti-tumor immune response that may be harnessed to improve the overall effectiveness and quality of cancer therapy. Previously, we also reported that induction of the cellular immune system was very important to suppress tumor metastasis.[35] Therefore, we believe that an induction of immune response is a significant benefit in ultrasound therapy.

In conclusion, the present study suggests that injection of BL in combination with low intensity ultrasound may be an effective cancer therapy. We provide evidence that these conditions stimulate the anti-tumor immune responses necessary for tumor growth regression.

Disclosure Statement

The authors have no conflict of interest to declare.

References

1 Kennedy JE. High-intensity focused ultrasound in the treatment of solid tumours. *Nat Rev Cancer* 2005; **5**: 321–7.
2 Bataineh O, Jenne J, Huber P. Clinical and future applications of high intensity focused ultrasound in cancer. *Cancer Treat Rev* 2012; **38**: 346–53.
3 Dubinsky TJ, Cuevas C, Dighe MK, Kolokythas O, Hwang JH. High-intensity focused ultrasound: Current potential and oncologic applications. *AJR Am J Roentgenol* 2008; **190**: 191–9.
4 Gelet A, Chapelon JY, Bouvier R et al. Transrectal high-intensity focused ultrasound: Minimally invasive therapy of localized prostate cancer. *J Endourol* 2000; **14**: 519–28.
5 Wu F, Wang ZB, Zhu H et al. Feasibility of US-guided high-intensity focused ultrasound treatment in patients with advanced pancreatic cancer: Initial experience. *Radiology* 2005; **236**: 1034–40.
6 Xiaoping L, Leizhen Z. Advances of high intensity focused ultrasound (HIFU) for pancreatic cancer. *Int J Hyperthermia* 2013; **29**: 678–82.
7 Coon J, Todd N, Roemer R. HIFU treatment time reduction through heating approach optimisation. *Int J Hyperthermia* 2012; **28**: 799–820.
8 Chung DJ, Cho SH, Lee JM, Hahn ST. Effect of microbubble contrast agent during high intensity focused ultrasound ablation on rabbit liver in vivo. *Eur J Radiol* 2012; **81**: e519–23.
9 Kaneko Y, Maruyama T, Takegami K et al. Use of a microbubble agent to increase the effects of high intensity focused ultrasound on liver tissue. *Eur Radiol* 2005; **15**: 1415–20.
10 Umemura S, Kawabata K, Sasaki K. In vivo acceleration of ultrasonic tissue heating by microbubble agent. *IEEE Trans Ultrason Ferroelectr Freq Control* 2005; **52**: 1690–8.
11 Shimamura M, Nakagami H, Taniyama Y, Morishita R. Gene therapy for peripheral arterial disease. *Expert Opin Biol Ther* 2014; **14**: 1175–84.
12 Fujishiro S, Mitsumori M, Nishimura Y et al. Increased heating efficiency of hyperthermia using an ultrasound contrast agent: a phantom study. *Int J Hyperthermia* 1998; **14**: 495–502.
13 Razansky D, Einziger PD, Adam DR. Enhanced heat deposition using ultrasound contrast agent–Modeling and experimental observations. *IEEE Trans Ultrason Ferroelectr Freq Control* 2006; **53**: 137–47.
14 Feril LB Jr, Kondo T. Biological effects of low intensity ultrasound: The mechanism involved, and its implications on therapy and on biosafety of ultrasound. *J Radiat Res* 2004; **45**: 479–89.
15 Hagisawa K, Nishioka T, Suzuki R et al. Thrombus-targeted perfluorocarbon-containing liposomal bubbles for enhancement of ultrasonic thrombolysis: in vitro and in vivo study. *J Thromb Haemost* 2013; **11**: 1565–73.
16 Hagisawa K, Nishioka T, Suzuki R et al. Enhancement of ultrasonic thrombus imaging using novel liposomal bubbles targeting activated platelet glycoprotein IIb∕IIIa complex–in vitro and in vivo study. *Int J Cardiol* 2011; **152**: 202–6.

17 Unga J, Hashida M. Ultrasound induced cancer immunotherapy. *Adv Drug Deliv Rev* 2014; **72**: 144–53.
18 Rychak JJ, Klibanov AL. Nucleic acid delivery with microbubbles and ultrasound. *Adv Drug Deliv Rev* 1999; **37**: 139–57.
19 Suzuki R, Takizawa T, Negishi Y, Utoguchi N, Maruyama K. Effective gene delivery with liposomal bubbles and ultrasound as novel non-viral system. *J Drug Target* 2007; **15**: 531–7.
20 Suzuki R, Takizawa T, Negishi Y et al. Tumor specific ultrasound enhanced gene transfer in vivo with novel liposomal bubbles. *J Control Release* 2008; **125**: 137–44.
21 Suzuki R, Oda Y, Utoguchi N et al. A novel strategy utilizing ultrasound for antigen delivery in dendritic cell-based cancer immunotherapy. *J Control Release* 2009; **133**: 198–205.
22 Suzuki R, Namai E, Oda Y et al. Cancer gene therapy by IL-12 gene delivery using liposomal bubbles and tumoral ultrasound exposure. *J Control Release* 2010; **142**: 245–50.
23 Hamano N, Negishi Y, Takatori K et al. Combination of Bubble liposomes and high-intensity focused ultrasound (HIFU) enhanced antitumor effect by tumor ablation. *Biol Pharm Bull* 2014; **37**: 174–7.
24 Castano AP, Mroz P, Hamblin MR. Photodynamic therapy and anti-tumour immunity. *Nat Rev Cancer* 2006; **6**: 535–45.
25 Liu HL, Hsieh HY, Lu LA, Kang CW, Wu MF, Lin CY. Low-pressure pulsed focused ultrasound with microbubbles promotes an anticancer immunological response. *J Transl Med* 2012; **10**: 221.
26 Honda H, Zhao QL, Kondo T. Effects of dissolved gases and an echo contrast agent on apoptosis induced by ultrasound and its mechanism via the mitochondria-caspase pathway. *Ultrasound Med Biol* 2002; **28**: 673–82.
27 Feril LB Jr, Kondo T, Zhao QL et al. Enhancement of ultrasound-induced apoptosis and cell lysis by echo-contrast agents. *Ultrasound Med Biol* 2003; **29**: 331–7.
28 Honda H, Kondo T, Zhao QL, Feril LB Jr, Kitagawa H. Role of intracellular calcium ions and reactive oxygen species in apoptosis induced by ultrasound. *Ultrasound Med Biol* 2004; **30**: 683–92.
29 Morris H, Rivens I, Shaw A, Haar GT. Investigation of the viscous heating artefact arising from the use of thermocouples in a focused ultrasound field. *Phys Med Biol* 2008; **53**: 4759–76.
30 Takeshima T, Chamoto K, Wakita D et al. Local radiation therapy inhibits tumor growth through the generation of tumor-specific CTL: Is potentiation by combination with Th1 cell therapy. *Cancer Res* 2010; **70**: 2697–706.
31 Xu ZL, Zhu XQ, Lu P, Zhou Q, Zhang J, Wu F. Activation of tumor-infiltrating antigen presenting cells by high intensity focused ultrasound ablation of human breast cancer. *Ultrasound Med Biol* 2009; **35**: 50–7.
32 Lu P, Zhu XQ, Xu ZL, Zhou Q, Zhang J, Wu F. Increased infiltration of activated tumor-infiltrating lymphocytes after high intensity focused ultrasound ablation of human breast cancer. *Surgery* 2009; **145**: 286–93.

33 Kanagawa N, Gao JQ, Motomura Y *et al.* Antitumor mechanism of intratumoral injection with IL-12-expressing adenoviral vector against IL-12-unresponsive tumor. *Biochem Biophys Res Commun* 2008; **372**: 821–5.

34 Xing Y, Lu X, Pua EC, Zhong P. The effect of high intensity focused ultrasound treatment on metastases in a murine melanoma model. *Biochem Biophys Res Commun* 2008; **375**: 645–50.

35 Oda Y, Suzuki R, Otake S *et al.* Prophylactic immunization with Bubble liposomes and ultrasound-treated dendritic cells provided a four-fold decrease in the frequency of melanoma lung metastasis. *J Control Release* 2012; **160**: 362–6.